Efficient removal of ciprofloxacin drug using electrospun of Co/Al-layered double hydroxide embedded chitosan/polyvinylidene fluoride nanofiber membrane

Table S1. Chemical name, formula, and company.

Chemical name	Formula	Company
Almunium chloride	$AlCl_3$	Sigma-Aldrich, Germany
Cobalt chloride	$CoCl_2$	Sigma-Aldrich, Germany
Chitosan (≥75% deacetylated having bulk a density of 0.15–0.3 g/cm3 and viscosity >200 Cp)	$C_{56}H_{103}N_9O_{39}$	isco Research Laboratory Pvt. Ltd (India)
Polyvinylidene fluoride	$-(C_2H_2F_2)_n-$	Sigma-Aldrich, Germany
Methanol	CH_3OH	LOBA CHEMIE PVT.LTD, India
Glacial acetic acid (purity 99.75%, AR)	$C_2H_4CO_2$	Sigma-Aldrich, Germany
Ethanol	C_2H_6O	Sigma-Aldrich, Germany
Sodium hydroxide (99%, AR)	NaOH	LOBA CHEMIE PVT.LTD, India
Hydrochloric acid (37%, AR)	HCl	LOBA CHEMIE PVT.LTD, India

Table S2. Instruments and equibments.

Test name	Abbrevation	Instrument name	Company	Illustration
Fourier transformer infrared	FT-IR	A Nicolet IS10 Fourier transform infrared (FTIR) spectrometer	Thermo Fisher Scientific, Waltham, MA, USA	equipped with an attenuated total reflectance accessory and which ran in the 4000-400 cm^{-1} range was used to gather FTIR spectra
Powered X-ray diffraction	PXRD	Siemens diffractometer (model D500, Germany)	Germany	patterns were captured from powder samples through the use of a Siemens diffractometer (model D500, Germany) that was fitted with a Cu-K radiation source (wavelength 1.54 Angstroms (Å)) operating at 30 kV and 20 mA.
Scanning Electron Microscope	SEM	(JSM-6510LV, JEOL Ltd., Tokyo, Japan)	JEOL Ltd., Tokyo, Japan	The morphology of the investigated sorbents was analyzed with the use of a scanning electron microscope
X-ray photoelectron spectroscopy	XPS	K-ALPHA (Themo Fisher Scientific, USA)	Themo Fisher Scientific, USA	Used for determination the elemental analysis for the compound
Braunnar Emmet Teller	BET	Quantachrome Instruments, Anton Paar Quanta Tec, Inc., Boynton Beach, FL, USA	Quanta Tec, Inc., Boynton Beach, FL, USA	was utilised for surface and pore analysis (Brunauer Emmett-Teller (BET) surface area, porous volume, and pore size), and NovaWin Software (v11.0) was used for data interpretation. The BET surface area of material adsorbents was

				obtained by the application of nitrogen adsorption-desorption isotherms at 77K through the use of a specific analyser (Quadrasorb–EVO, Quantachrome, USA).
UV-visible Spectrophotometer	UV-Vis.	Jasco V-630	Japan	Measuring the concentration of the adsorbate soulution.
pH meter	pH	HANNA (model 211)	USA	Measuring the acidity or basicity of the solution
Sonication	Ultrasonic	Elmasonic P300H ultrasonic bath, continuous mode, power 380 W	Elma Schmidbauer GmbH, Singen, Germany	Sonication of the material as well as used ton disperse material on the solution as it decrease the particle size of the material
Water bath	Shaking	GFL Orbital Shaker 3017		

Table S3. True variables, codes, and their BBD levels.

Code	**Variables**	**-1**	**0**	**+1**
A	pH	2	7	12
B	Dose (g)	0.02	0.26	0.5
C	Time (min.)	5	55.5	100

Table S4. Equations used in this work to fit the data of adsorption experiments.

Serial	Equation	Nmae	Description	Ref.
1	$q_e = \frac{q_m}{1 + K_L C_e}$	Langmuir	q_e ($mg.g^{-1}$) Adsorption capacity, C_e equilibrium concentration, q_m ($mg.g^{-1}$) is the monolayer saturation capacity constant and K_L (L/mg) is the Langmuir constant associated with the free adsorption energy. The favorability of the adsorption process in the Langmuir model is determined by means of the R_L dimensionless factor ($R_L = 1/(1 + k_L \cdot C_0)$) as follows: $R_L = 0$, $0 < R_L < 1$, $R_L = 1$, and $R_L > 1$ indicating irreversible, favorable, linear, and unfavorable adsorption isotherms, respectively.	[1]
2	$q_e = K_F C_e^{\frac{1}{n}}$	Freundlich	K_F Freundlich isotherm constants $[(mg/g)/(mg/L)^{1/n}]$, and $1/n$ represents the exponent of non-linearity (i.e., C-type, L-type, and S-type isotherms). n is the Freundlich constants, and $n < 1$ indicates poor adsorption while $n = 1–2$ and $n = 2–10$ indicate average and good adsorptions, respectively. The values of n and k_f are calculated, respectively	[2]
3	$q_e = q_m \exp(-\beta\varepsilon^2)$ $\varepsilon = RT ln\left(1 + \frac{1}{C_e}\right)$ $E_{DR} = \sqrt{\frac{1}{2K_{DR}}}$	Dubinin–Radushkevich	q_D is the maximum monolayer adsorption capacity (mg/g), B_D is the activity coefficient related to the apparent free energy of adsorbate adsorption onto the adsorbent (mol^2/kJ^2), ε_D is the Polanyi potential which is related to the equilibrium concentration, and E is the mean adsorption energy.	[3]

4	$q_e = Q_{max}\frac{RT}{b}\ln(K_T C_e)$	Temkin	K_T is the Temkin isotherm constant or equilibrium binding constant (L/mg) corresponding to the maximum binding energy, and b_T is the Temkin isotherm constant related to the heat of adsorbate adsorption onto the adsorbent due to adsorbent-adsorbate interaction (J/mol), R is the gas constant (8.314 J/mol.K), and T is the absolute temperature (herein 298 K).	[4]
5	$q_t = q_e\left(1 - e^{K_1 t}\right)$	Pseudo-First-order kinetic	q_e and q_t are the adsorption capacities at equilibrium and time t (mg/g), and k_1 is the rate constant (min^{-1}), respectively.	[5]
6	$q_t = \frac{tK_2 q_e^2}{1 + q_e K_2 t}$	Pseudo-Second-order kinetic	k_2 is the pseudo-second order constant (mg/(g.min))	[6]
7	$q_t = K_i t^{1/2} + X$	Intraparticle diffusion	q_t is the adsorption capacity at time t in (mg/g), k_{int} is the intraparticle diffusion rate constant ($mg \cdot g^{-1} min^{-1/2}$), and C is a constant related to the the thickness of the boundary layer (mg/g).	[7]
8	$q_t = \frac{1}{\beta}\ln(\alpha\beta t + 1)$	Elovich	The constants α chemical adsorption rate ($mg.g^{-1}min^{-1}$), and β Coefficient in relation with extension of covered surface	[8]
9	$\Delta G^o = \Delta H^o - T\Delta S^o$	Gibbs free energy	ΔG°: Gibbs free energy change; K_d: equilibrium constant; R: gas constant; T: temperature.	[9]
10	$lnK_d = \frac{\Delta S^\circ}{R} - \frac{\Delta H^\circ}{RT}$	Van’t Hoff	ΔS°: entropy change; ΔH°: enthalpy change.	[10]
11	$lnK_d = lnA - (\frac{Ea^0}{R})\frac{1}{T}$	Arrhenius	Ea was the activation energy, A Arhinus constant, R ideal gas constant 8.314 J/mol.K, T (K) is the absolute solution temperature	[11]

Table S5. The parameter of the adsorption isotherm for CIP onto Co/Al-LDH-CS/PVDF nanofiber membrane and CS/PVDF nanofiber membrane .

Isotherm	Value of parameters	Co/Al LDH CS/PVDF nanofiber membrane	CS/PVDF nanofiber membrane
Langmuir	$q_{m\ exp}$ (mg/g)	352.6	289.8
	q_m (mg/g)	354.5	292.6
	K_L (L/mg)	0.0446	0.4035
	R_L	0.48	0.36
	Reduced Chi-Sqr	96.0754	71.81092
	Residual Sum of Squares	1441.13103	1148.97464
	R-Square (COD)	0.99233	0.99282
	R^2	0.99182	0.99237
Freundlich	n	2.65	2.6
	K_F (mg/g) $(L/mg)^{1/n}$	59.03	47.920
	Reduced Chi-Sqr	1003.49535	694.19242
	Residual Sum of Squares	16055.92553	11107.07864
	R-Square (COD)	0.93218	0.93059
	R^2	0.92794	0.92625
Dubinin–Radushkevich	Q_{DR}($mg.g^{-1}$)	325.35	266.92
	K_{DR} ($mol^2k\ J^{-2}$)	2.27E-5	2.31E-5
	Ea (kJ/mol)	31.8	29.84
	Reduced Chi-Sqr	865.84775	577.38824
	Residual Sum of Squares	13853.56404	9238.21191
	R-Square (COD)	0.94148	0.94227
	R^2	0.93782	0.93866
Temkin	b_T (J/mol)	27.928	23.89
	K_T (L/mol)	0.45	0.41

	Reduced Chi-Sqr	220.27827	161.86859
	Residual Sum of Squares	3524.4523	2589.8975
	R-Square (COD)	0.98511	0.98381
	R^2	0.98418	0.9828
Jossens	K	15.015	12.07
	J	0.017	0.016
	Reduced Chi-Sqr	36.39689	32.04771
	Residual Sum of Squares	545.95336	480.71562
	R-Square (COD)	0.99769	0.997
	R^2	0.99739	0.9966

Table S6. Models of adsorption kinetic parameters of CIP onto Co/Al-LDH-CS/PVDF nanofiber membrane and CS/PVDF nanofiber membrane .

Model	Value of parameters	Co/Al LDH CS/PVDF nanofiber membrane	CS/PVDF nanofiber membrane
Pseudo-First-order kinetic	K_1 (min^{-1})x10^{-2}	0.18	0.168
	Reduced Chi-Sqr	430.3976	694.25213
	Residual Sum of Squares	8177.55449	12496.53842
	R-Square (COD)	0.97029	0.91638
	R^2	0.96873	0.91174
Pseudo-second-order kinetic	K_2 (g.mg^{-1}min^{-1})x10^{-2}	6.4E-4	9.17E-4
	q_e (mg/g)	355.45	291.6
	Reduced Chi-Sqr	189.16422	459.59917
	Residual Sum of Squares	3594.12014	8272.78512
	R-Square (COD)	0.98694	0.94464
	R^2	0.98625	0.94157

Intraparticle diffusion	K_i (mg.g^{-1}min$^{1/2}$)	35.37	26.38
	X (mg/g)	85.80	82.57
	Reduced Chi-Sqr	3197.85057	1838.16881
	Residual Sum of Squares	60759.16081	33087.03865
	R-Square (COD)	0.77925	0.77861
	R^2	0.76763	0.76631
Elovich	β (g/mg)	66.67	41.17
	α (mg.g^{-1}min^{-1})	0.05	0.03
	Reduced Chi-Sqr	463.52993	605.95874
	Residual Sum of Squares	8807.06864	10907.25737
	R-Square (COD)	0.968	0.92702
	R^2	0.96632	0.92296
Experimental data	q_e (exp) (mmol/g)	354.6	292.4

Table S7. The thermodynamic parameters.

T (K)	ΔG (kJ/mol)	ΔH (kJ/mol)	Ea (kJ/mol)	ΔS (J/mol.K)
293	-0.392338			
298	-1.00441	83.62	36.82	282.65
303	-2.40117			
308	-3.79792			
313	-5.19467			
318	-6.59142			

Table S8. Comparison of adsorbent adsorption capacity of antibiotics.

Material	Q_{max}(mg.g^{-1})	References
P-CNT3	28.6	[12]
Graphene oxide/calcium alginate biocomposite	39.6	[13]
Natural bentonite (BSN)	294	[14]

Biochar (Fe-modified bamboo)	153.8	[15]
chitosan-CNT	23.7	[16]
ZnCo-ZIF@CS	348.9	[17]
Fe/N-BC	46.45	[18]
Co/Al-LDH-CS/PVDF	352.6	This search

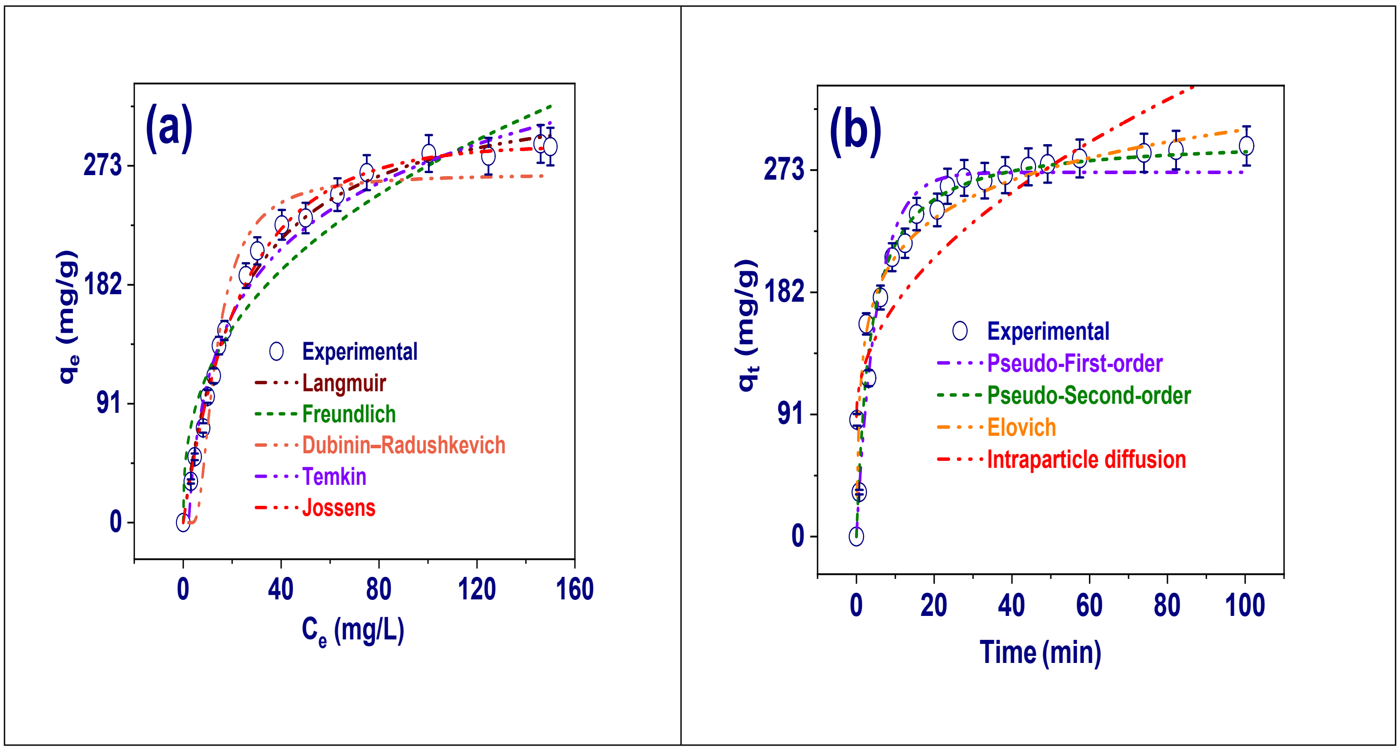

Fig. S1. (a) The models of adsorption isotherms of CS/PVDF, (b) The models of adsorption kinetics of CS/PVDF,

References

[1] I. Langmuir, The constitution and fundamental properties of solids and liquids. Part I. Solids, J. Am. Chem. Soc., 38 (1916) 2221-2295.

[2] H.M.F. Freundlich, Over the adsorption in solution, J. Phys. Chem., 57 (1906) 385-471.

[3] M. Dubinin, The equation of the characteristic curve of activated charcoal, Proc. Acad. Sci. USSR Phys. Chem. Sect., 55 (1947) 327-329.

[4] V.P. M.I. Tempkin, Kinetics of ammonia synthesis on promoted iron catalyst, Acta Phys. Chim. USSR, 12 (1940) 327-356.

[5] S.K. Lagergren, About the theory of so-called adsorption of soluble substances, Sven. Vetenskapsakad. Handingarl, 24 (1898) 1-39.

[6] Y.-S. Ho, G. McKay, Sorption of dye from aqueous solution by peat, Chemical engineering journal, 70 (1998) 115-124.

[7] W.J. Weber Jr, J.C. Morris, Kinetics of adsorption on carbon from solution, J. Sanit. Eng. Div., 89 (1963) 31-59.

[8] M.H. Dehghani, A. Dehghan, A. Najafpoor, Removing Reactive Red 120 and 196 using chitosan/zeolite composite from aqueous solutions: Kinetics, isotherms, and process optimization, Journal of Industrial and Engineering Chemistry, 51 (2017) 185-195.

[9] E.C. Lima, A. Hosseini-Bandegharaei, J.C. Moreno-Piraján, I. Anastopoulos, A critical review of the estimation of the thermodynamic parameters on adsorption equilibria. Wrong use of equilibrium constant in the Van't Hoof equation for calculation of thermodynamic parameters of adsorption, Journal of molecular liquids, 273 (2019) 425-434.

[10] H.N. Tran, S.-J. You, A. Hosseini-Bandegharaei, H.-P. Chao, Mistakes and inconsistencies regarding adsorption of contaminants from aqueous solutions: a critical review, Water research, 120 (2017) 88-116.

[11] B. Oladipo, E. Govender-Opitz, T.V. Ojumu, Kinetics, thermodynamics, and mechanism of Cu (II) ion sorption by biogenic iron precipitate: using the lens of wastewater treatment to diagnose a typical biohydrometallurgical problem, ACS omega, 6 (2021) 27984-27993.

[12] A.H. Khan, H.A. Aziz, P. Palaniandy, M. Naushad, N. Zouli, Ciprofloxacin adsorption onto CNT loaded pumice: adsorption modelling, kinetics, equilibriums and reusability studies, Journal of Molecular Liquids, 399 (2024) 124388.
[13] C. Li, X. Li, N. Graham, A study of the preparation and reactivity of potassium ferrate, Chemosphere, 61 (2005) 537-543.
[14] L. Jara-Cobos, D. Abad-Delgado, J. Ponce-Montalvo, M. Menendez, M.E. Peñafiel, Removal of ciprofloxacin from an aqueous medium by adsorption on natural and hydrolyzed bentonites, Frontiers in Environmental Science, 11 (2023) 1239754.
[15] W.K. Wakejo, B.T. Meshasha, J.W. Kang, Y. Chebude, Enhanced ciprofloxacin removal from aqueous solution using a chemically modified biochar derived from bamboo sawdust: adsorption process optimization with response surface methodology, Adsorption Science & Technology, 2022 (2022) 2699530.
[16] S.M. Khumalo, B.F. Bakare, S. Rathilal, Single and multicomponent adsorption of amoxicillin, ciprofloxacin, and sulfamethoxazole on chitosan-carbon nanotubes hydrogel beads from aqueous solutions: Kinetics, isotherms, and thermodynamic parameters, Journal of Hazardous Materials Advances, 13 (2024) 100404.
[17] Q. Luo, P. Liu, L. Bi, L. Shi, J. Zhou, F. Fang, Q. Lv, H. Fu, X. Li, J. Li, Selective and efficient removal of ciprofloxacin from water by bimetallic MOF beads: Mechanism quantitative analysis and dynamic adsorption, Separation and Purification Technology, 332 (2024) 125832.
[18] B. Yao, W. Zeng, A. Núñez-Delgado, Y. Zhou, Simultaneous adsorption of ciprofloxacin and Cu2+ using Fe and N co-doped biochar: Competition and selective separation, Waste Management, 168 (2023) 386-395.